

## Geometry and Physics of Wrinkling

E. Cerda<sup>1,2</sup> and L. Mahadevan<sup>1,\*</sup>

<sup>1</sup>*Department of Applied Mathematics and Theoretical Physics, University of Cambridge, Silver Street, Cambridge CB3 9EW, United Kingdom*

<sup>2</sup>*Departamento de Física, Universidad de Santiago de Chile, Avenida Ecuador 3493, Casilla 307, Correo 2, Santiago, Chile*  
(Received 25 June 2002; published 19 February 2003)

The wrinkling of thin elastic sheets occurs over a range of length scales, from the fine scale patterns in substrates on which cells crawl to the coarse wrinkles seen in clothes. Motivated by the wrinkling of a stretched elastic sheet, we deduce a general theory of wrinkling, valid far from the onset of the instability, using elementary geometry and the physics of bending and stretching. Our main result is a set of simple scaling laws; the wavelength of the wrinkles  $\lambda \sim K^{-1/4}$ , where  $K$  is the stiffness due to an “elastic substrate” effect with a multitude of origins, and the amplitude of the wrinkle  $A \sim \lambda$ . These could form the basis of a highly sensitive quantitative wrinkling assay for the mechanical characterization of thin solid membranes.

DOI: 10.1103/PhysRevLett.90.074302

PACS numbers: 46.32.+x, 46.70.De, 47.54.+r

The depiction of wrinkles in art is as old as the subject itself. However, the scientific study of wrinkles is a much more recent subject as it involves the large deformations of naturally thin flat sheets whose behavior is governed by a set of nonlinear partial differential equations, known as the Föppl–von Karman equations [1]. They are essentially impossible to solve in analytical form except in some one-dimensional cases, so that one has to resort to either computations or a semianalytical approach using scaling and asymptotic arguments to make progress. Here, we use the latter approach to quantify the wrinkling of a thin elastic sheet which deforms under the influence of external forces and/or geometrical constraints. Our results complement those of classical tension-field theory [2–4], which focuses on the much simpler problem of determining the location of the wrinkles by using the linearized in-plane elastic response and neglecting the bending resistance of the sheet.

To illustrate the main ideas, we consider a simple example of wrinkling seen in a stretched, slender elastic sheet cut out of a polyethylene sheet. This must be contrasted with the crumpling of the same sheet [5,6], where the sheet responds by bending almost everywhere, and stretching is limited to a few boundary layers in the vicinity of peaks and ridges. When such a thin isotropic elastic sheet of thickness  $t$ , width  $W$ , length  $L$  ( $t \ll W \ll L$ ) made of a material with Young’s modulus  $E$  and Poisson’s ratio  $\nu$  is subject to a longitudinal stretching strain  $\gamma$  in its plane, it stays flat for  $\gamma < \gamma_c$ , a critical stretching strain. Further stretching causes the sheet to wrinkle, as shown in Fig. 1. This nonintuitive behavior arises because the clamped boundaries prevent the sheet from contracting laterally in their vicinity setting up a local biaxial state of stress; i.e., the sheet is sheared near the boundaries. Because of the symmetry in the problem, an element of the sheet near the clamped boundary, but away from its center line, will be unbalanced in the absence of a transverse stress because of the biaxial

deformation. This transverse stress is tensile near the clamped boundary and compressive slightly away from it [7,8]. When  $\gamma \sim \gamma_c$ , the sheet buckles to accommodate the in-plane strain incompatibility generated via the Poisson effect. For the sheet shown in Fig. 1,  $\gamma \approx 10^{-2}$ . This is well within the elastic limit, confirming the observation that thin sheets wrinkle easily in tension and/or shear. However, typically  $\gamma \gg \gamma_c$ , so that a linear theory is of little use and we must consider the geometrically nonlinear behavior of the wrinkles.

For a sheet so stretched, a periodic texture of parallel wrinkles decorates most of the sheet. To determine the criterion for the selection of the wavelength and the amplitude of the wrinkles, we must account for the energetic cost of bending and stretching. Additionally any geometric constraints must be imposed using Lagrange multipliers. We assume that the out-of-plane displacement of the initially flat sheet of area  $WL$  is  $\zeta(x, y)$ , where  $x \in (0, L)$  is the coordinate along the sheet measured from one end and  $y \in (0, W)$ ,  $W \ll L$  is the coordinate perpendicular to it measured from its central axis. Then we write the functional to be extremized as

$$\mathcal{U} = U_B + U_S - \mathcal{L}. \quad (1)$$

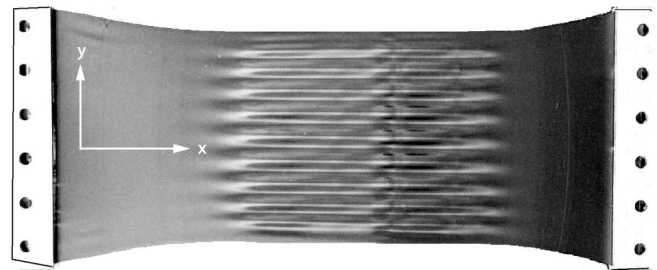


FIG. 1. Wrinkles in a polyethylene sheet of length  $L \approx 25$  cm, width  $W \approx 10$  cm, and thickness  $t \approx 0.01$  cm under a uniaxial tensile strain  $\gamma \approx 0.10$ . (Figure courtesy of K. Ravi-Chandar)

Here  $U_B = \frac{1}{2} \int_A B(\partial_y^2 \zeta)^2 dA$  is the bending energy due to the deformations which are predominantly in the  $y$  direction [9], where  $B = Et^3/[12(1 - \nu^2)]$  is the bending stiffness and  $U_S = \frac{1}{2} \int_A T(x)(\partial_x \zeta)^2 dA$  is the stretching energy [10] in the presence of a tension  $T(x)$  along the  $x$  direction [11]. As the sheet wrinkles in the  $y$  direction under the action of a small compressive stress, it satisfies the condition of inextensibility,

$$\int_0^L \left[ \frac{1}{2} (\partial_y \zeta)^2 - \frac{\Delta(x)}{W} \right] dy = 0. \quad (2)$$

This constraint is embodied in the final term in (1),  $\mathcal{L} = \int_A b(x)[(\partial_y \zeta)^2/2 - \Delta(x)/W] dA$ , where  $b(x)$  [12] is the unknown Lagrange multiplier and  $\Delta(x)$  is the imposed compressive transverse displacement. The Euler-Lagrange equation obtained from the condition of a vanishing first variation of (1),  $\delta U/\delta \zeta = 0$ , yields

$$B\partial_y^4 \zeta - T(x)\partial_x^2 \zeta + b(x)\partial_y^2 \zeta = 0. \quad (3)$$

For the example of the stretched sheet,  $T(x) \sim Eh\gamma = \text{const}$ , while  $\Delta(x) \sim \nu\gamma W = \text{const}$  far from the clamped boundaries, so that  $b(x) = \text{const}$ . Away from the free edges, the wrinkling pattern is periodic so that  $\zeta(x, y) = \zeta(x, y + 2\pi/k_n)$ , where  $k_n = 2\pi n/W$ , and  $n$  is the number of wrinkles [13]. At the clamped boundaries,  $\zeta(0, y) = \zeta(L, y) = 0$  [9]. Substituting a periodic solution of the form  $\zeta = \sum_n e^{ik_n y} X_n(x)$  into (3) yields a Sturm-Liouville-like problem

$$\frac{d^2 X_n}{dx^2} + \omega_n^2 X_n = 0, \quad X_n(0) = X_n(L) = 0, \quad (4)$$

where  $\omega_n^2 = (bk_n^2 - Bk_n^4)/T$ . Here, the compressive force  $b(x)$  is determined by the nonlinear constraint (2) so that the effective potential associated with (4) is *a priori* unknown. The solution to (4) when  $b \sim \text{const}$  is  $X_n = A_n \sin \omega_n x$ ,  $\omega_n = m\pi/L$ . Since the solution with least bending energy corresponds to  $m = 1$ , we have  $\omega_n = \pi/L$  so that  $b_n(k_n) = \frac{\pi^2 T}{L^2 k_n^2} + Bk_n^2$  and  $\zeta = A_n \cos(k_n y + \phi_n) \sin \pi x/L$ . Plugging this into (2) yields  $A_n^2 k_n^2 W/8 \approx \Delta$ , relating the wave number and the amplitude, so that finally we may write  $\mathcal{U} = Bk_n^2 \Delta L + \pi^2 T \Delta/k_n^2 L$ . The wavelength  $\lambda = 2\pi/k$  and the amplitude  $A$  are obtained by minimizing  $\mathcal{U}$  and using (2),

$$\lambda = 2\sqrt{\pi} \left( \frac{B}{T} \right)^{1/4} L^{1/2}, \quad A = \frac{\sqrt{2}}{\pi} \left( \frac{\Delta}{W} \right)^{1/2} \lambda. \quad (5)$$

For the stretched sheet, this yields  $\lambda = (2\pi L t)^{1/2}/[3(1 - \nu^2)\gamma]^{1/4}$ ,  $A = (\nu L t)^{1/2}/[16\gamma/3\pi^2(1 - \nu^2)]^{1/4}$ , which results have been quantitatively verified by experiments [14]. We observe that as  $\nu \rightarrow 0$ , the wrinkle amplitude  $A \rightarrow 0$ , although the wavelength remains unchanged. However, this dependence of  $\Delta(x)$  on  $\nu$  is incidental, as any geometric packing constraint suffices to induce wrinkling. Although the wrinkles are engendered by the weak compressive stresses near the clamped boundaries, they

extend over the entire domain. To understand this, we consider the persistence length  $L_d$  of a wrinkle, defined as the distance over which a sheet pinched at one end with an amplitude  $\zeta$  and width  $\lambda_d$  eventually flattens out. Balancing the stretching and bending energies over the area  $\lambda_d L_d$  yields  $U_B \sim B\zeta^2 L_d/\lambda_d^3 \sim U_S \sim Eh\gamma\zeta^2 \lambda_d/L_d$  so that  $L_d \sim \lambda_d^2 \gamma^{1/2}/t$ . If  $\lambda_d \sim \lambda$ ,  $L_d \sim L$ ; i.e., the wrinkles persist over the entire domain.

We now give a physical interpretation of the mechanism for the selection of the wrinkle wavelength. The form of  $U_B$  in (1) makes it transparent that the total energy increases rapidly for short wavelengths. The expression for the stretching energy  $U_S \sim \frac{1}{2} \int_A T(\partial_x \zeta)^2 dA$  in (1) is analogous to the form of the energy in an elastic foundation supporting a thin sheet,  $U_F \sim \frac{1}{2} \int_A K\zeta^2 dA$ , where  $K$  is the stiffness of the foundation. Comparing the two, we see that  $K \sim T/L^2$  is the stiffness of the “effective” elastic foundation for the stretched sheet. Then the total energy also increases with long wavelengths due to the increase in the longitudinal stretching strain. This effect arises directly from the geometrical constraint of inextensibility in the transverse direction: a larger wavelength increases the amplitude of the wrinkles, so that it must also be stretched much more longitudinally. A similar effect is seen in a sheet supported on a real elastic foundation [1], where a longitudinal compressive stress field combined with the constraint of longitudinal inextensibility leads to an increase in energy for long wavelengths. In either case, the balance between the foundation and bending energies leads to the selection of wrinkles of an intermediate wavelength, as in (5) which we may rewrite as

$$\lambda \sim \left( \frac{B}{K} \right)^{1/4}, \quad A \sim \left( \frac{\Delta}{W} \right)^{1/2} \lambda. \quad (6)$$

These expressions make transparent the ingredients for all wrinkling phenomena: a thin sheet with a bending stiffness  $B$ , an effective elastic foundation of stiffness  $K$ , and an imposed compressive strain  $\Delta/W$ . The geometric packing constraint leads to the formation of wrinkles, the bending resistance of the sheet penalizes short wavelength wrinkles, while an effective elastic foundation supporting the sheet penalizes long wavelengths, thus leading to the generation of new intermediate length scales. Since the actual form of  $K$  (or  $T$ ) and  $\Delta$  will vary from one problem to another, (6) leads to a variety of different scalings.

The wrinkling of the skin of a shriveled apple [Fig. 2(a)] provides a first tractable testbed for our general theory. Here, the wrinkles arise due to the compression induced by the drying of the flesh, which is an elastic substrate of thickness  $H_s$  and Young’s modulus  $E_s$ . The wavelength is determined by a competition between the effect of the flesh which resists large wavelength deformations, and the bending stiffness of the skin which prevents short wavelength deformations. In this situation, the stiffness of the substrate  $K = E_s f(\lambda/l_p)/l_p$ , where  $l_p$

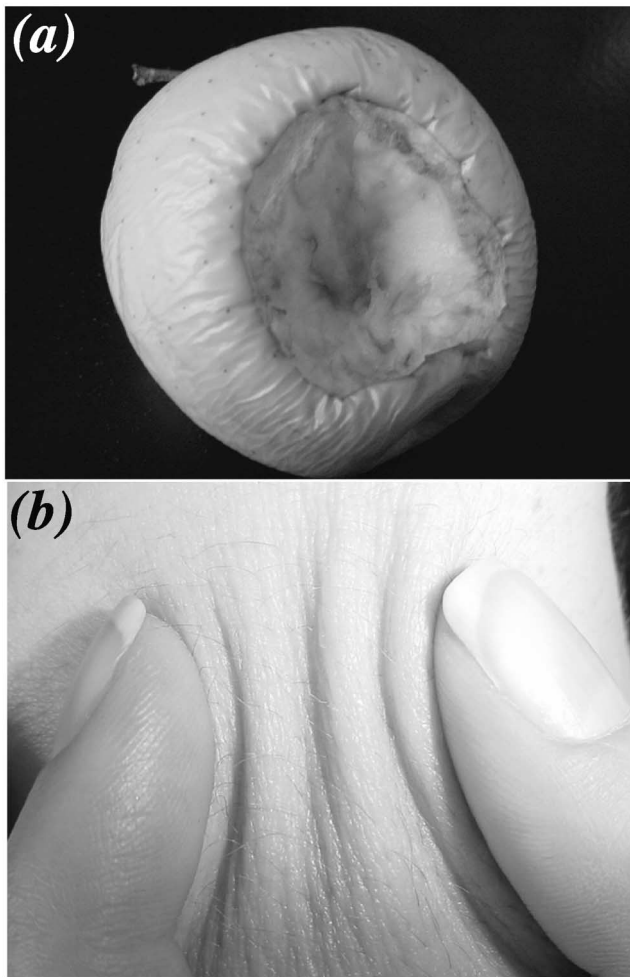


FIG. 2. Wrinkling of skin. (a) Wrinkles induced in the skin of an apple ( $\approx 5$  cm) by the shrinking of the flesh. Observe that the wrinkles are orthogonal to the free boundary where the drying first starts. (b) Compression wrinkles induced on the back of one's hand by bunching up the skin + substrate. The wavelength in such a situation is predicted to scale as the thickness of the layer, consistent with observations.

is a characteristic penetration length of the deformation and  $f(\lambda/l_p)$  is a dimensionless function that depends on the geometry of the system. For an incompressible substrate, the horizontal deformation scales as  $\zeta\lambda/l_p$ . Then the dominant shear strain scales as  $\gamma \sim \zeta\lambda/l_p^2$  and the elastic energy density (per unit area) of the substrate scales as  $E_s l_p \gamma^2 \sim E_s \lambda^2 / l_p^3 \zeta^2$ . Therefore,  $f(\lambda/l_p) \sim \lambda^2 / l_p^2$ , so that the effective stiffness of the substrate is  $K \sim E_s \lambda^2 / l_p^3$ . In general, there are two main types of wrinkles: compression wrinkles which arise in a one-dimensional stress field (induced, say, by muscles) when the substrate is relatively stiff, i.e.,  $K \gg T/L^2$ , and tension wrinkles which arise in a truly two-dimensional stress field in more subtle way (due to pre-stress, geometry, and muscular action) when  $K \ll T/L^2$ . However, in both cases, the constraint of inextensibility is crucial in determining the fine structure of the wrinkles (6). For the

shrinkage-induced wrinkles in Fig. 2(a), the wavelength  $t \ll \lambda \ll H_s$ , and so the wrinkles on the skin decay exponentially into the bulk. In this deep substrate limit,  $l_p \sim \lambda$ . Then  $K \sim E_s / \lambda$ , and the wrinkle wavelength  $\lambda \sim (B/K)^{1/4}$  giving  $\lambda \sim t(E/E_s)^{1/3}$  [15]. For the apple [Fig. 2(a)], we estimate  $E/E_s \sim 10$  [16], which yields  $\lambda \sim 3t$ . For  $t \approx 0.5$  mm,  $\lambda \approx 1.5$  mm, qualitatively consistent with our observations.

We now turn to the wrinkling of our skin [Fig. 2(b)], where a thin, relatively stiff epidermis is attached to a soft dermis which is typically 10 times thicker [17]. The wrinkled appearance of aging skin is a consequence of many factors including the degradation of its mechanical properties, the existing pre-stress, and the action of the underlying muscles. While much still needs to be done to understand the detailed effects of these determinants on wrinkling, here we sketch a simple geometric picture of the phenomenon. Over much of the body, this composite layer sits atop a deep soft connective tissue so that the effect of wrinkling is minimal. However, wrinkling is prominent in regions where (a) there is excess skin and/or (b) the skin is close to the bony skeleton and drapes it. Here, the presence of a pre-stress can lead to tension wrinkles, seen in the elbows and knees, while the action of muscles can lead to compression wrinkles, seen in the furrowing of one's brow, although the two effects can act in concert as in the crow's feet patterns radiating from the eye. In these cases, the skin rests on a shallow elastic substrate, and  $\lambda \gg H_s \gg t$  which gives the penetration length  $l_p \sim H_s$ , and  $K \sim E_s \lambda^2 / H_s^3$ . The wrinkle wavelength in such cases is  $\lambda \sim (tH_s)^{1/2} (E/E_s)^{1/6}$ . For human skin,  $E/E_s \sim 10^3$  and  $H_s/t \sim 10$  so that  $\lambda \approx H_s$ . A quick check of this estimate may be performed by pinching the back of one's hand to determine  $2H_s \approx 5$  mm giving  $\lambda \approx 2.5$  mm for a simple experiment [Fig. 2(b)]. This is in the right range and could provide a quantitative guide to the empirical art of measuring the anisotropy of skin tautness.

Our results could form the basis of a quantitative wrinkling assay for the mechanical characterization of thin solid films. The field of wrinkles generated by a cell crawling on a soft substrate [Fig. 3(a)] [18,19] have long been used as a qualitative assay of the forces generated during cell movement. The scaling law (5) now makes this quantitative. Inverting (5) yields  $T \sim BL^2/\lambda^4$  and indicates that the wavelength measurements could be an extremely sensitive technique for the characterization of a distributed force field. The shear-induced wrinkling of polymerized vesicles [Fig. 3(b)] used for drug delivery and as artificial red blood cells [20] suggests a different assay; here the wrinkles may be used to deduce the bending stiffness of the membrane, a critical parameter in determining the robustness of these vesicles as they move through capillaries. Indeed, rewriting (5) yields  $B = T\lambda^4/16\pi^2 L^2$ . Using the data given in [21], we find that  $B \approx 4.6 \times 10^{-17}$  Nm. With the additional information about the in-plane modulus which is easier to

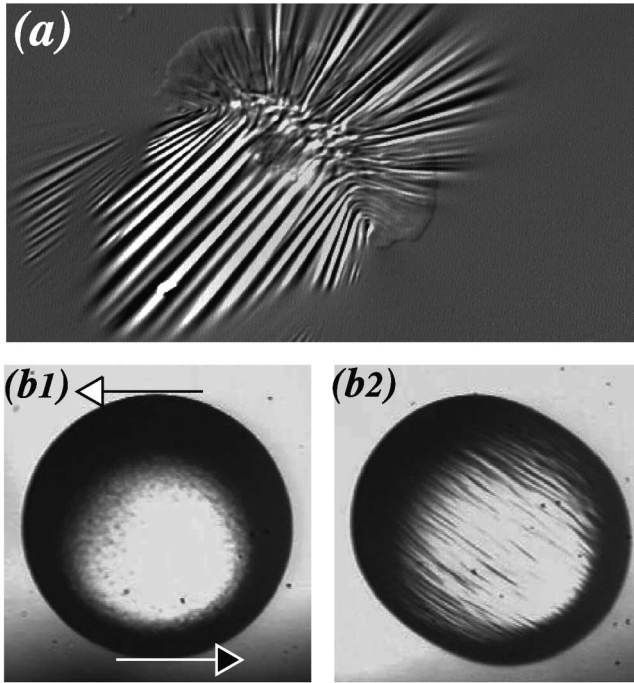


FIG. 3. The basis for wrinkling assays of thin solid films. (a) Wrinkles on a thin elastic substrate induced by the forces exerted by a cell (figure courtesy of K. Burton, reprinted from [19] with permission by the American Society of Cell Biology). Typical wavelengths are in the range of  $\mu\text{m}$ , and lengths are in the range of  $10 \mu\text{m}$ . (b) Wrinkles on a vesicle ( $\approx 10 \mu\text{m}$  that is solid in its plane; observe that the wrinkles appear at  $45^\circ$  to the direction to flow-induced shear, corresponding to the direction of maximum compression (figure courtesy of H. Rehage, reprinted from [20] with permission of Elsevier Science).

measure, it may be possible to monitor the vesicle thickness as a function of the polymerization index. For example, using our bending stiffness just calculated and the in-plane modulus in [21] gives the thickness of the vesicle in Fig. 3(b) as  $43 \text{ nm}$ .

We conclude by pointing out that our analysis may be formalized by a singular perturbation analysis of the Föppl–von Karman equations, which lead to (3) naturally [21]. This opens up various generalizations to include the effects of anisotropy (e.g., textiles), non-Hookean material behavior (e.g., elastomers and viscous liquids), etc. Indeed, we can even expect wrinkles in a rapidly stretched flat viscous sheet, just as they have been observed in compressed curved ones [22]. But once again, the essence is in the geometry.

E. C. acknowledges the support of Fundación Andes, of Universidad de Santiago DICYT project “The table cloth problem” (1999–2001), of Fondecyt 1020359 (2002), and of Fondap 11980002 (2002). L. M. acknowledges the support of ENS-Paris through a Chaire Condorcet (2001), of ESPCI-Paris through a Chaire Paris Sciences (2001) during the preliminary phase of this work, and of the U.S. National Institutes of Health and the Office of Naval Research for continuing support.

\*Electronic address: l.mahadevan@damtp.cam.ac.uk

- [1] L. Landau and E. M. Lifshitz, *Theory of Elasticity* (Pergamon, New York, 1986), 3rd ed.
- [2] H. Wagner, *Z. Flugtech. Motorluftschiffart*, **20**, Nos. 8–12 (1929).
- [3] E. H. Mansfield, in *Proceedings of the XIIth International Congress on Theoretical and Applied Mechanics* (Springer-Verlag, New York, 1968).
- [4] D. J. Steigmann, *Proc. R. Soc. London A* **429**, 141 (1990).
- [5] A. Lobkovsky, S. Gentges, H. Li, D. Morse, and T. Witten, *Science* **270**, 1482 (1995).
- [6] E. Cerda, S. Chaieb, F. Melo, and L. Mahadevan, *Nature (London)* **401**, 46 (1999).
- [7] J. Benthem, *Q. J. Mech. Appl. Math.* **16**, 413 (1963).
- [8] N. Freidl, F. G. Rammerstorfer, and F. D. Fischer, *Comput. Struct.*, **78**, 185 (2000).
- [9] Although  $U_B = \frac{1}{2} \int B(\Delta \zeta)^2 dA$ , the dominant term in the energy is  $\frac{1}{2} \int B(\partial_y^2 \zeta)^2 dA$  because of the short wavelength wrinkles in the  $y$  direction. Since the resulting Euler-Lagrange equation is then only second order in  $x$ , we cannot satisfy  $\partial_x \zeta = 0$  at the two ends  $x = 0, L$  in this simplified theory. In fact, the boundary layer size is  $O(W) \ll L$ , so that our theory is valid over most of the sheet, except near the clamped boundaries, as Fig. 1 shows.
- [10] This contribution is analogous to the energy stored in a string under tension when it is plucked.
- [11] Here and elsewhere, we keep terms to order  $O(\zeta^2)$ .
- [12] The Lagrange multiplier  $b(x)$  physically denotes a transverse force/length in the  $y$  direction. Then  $b(x) > 0$ ; i.e., the constraint is imposed by a compressive force/length.
- [13] The assumption of periodicity is exact if we were stretching a cylindrical sheet. For a flat sheet, the assumption of periodicity is only approximate, but the edge effects are small and may be safely neglected here.
- [14] E. Cerda, K. Ravi-Chandar, and L. Mahadevan, *Nature (London)* **419**, 579 (2002).
- [15] N. Bowden, S. Brittain, A. G. Evans, J. W. Hutchinson, and G. M. Whitesides, *Nature (London)*, **393**, 146 (1998).
- [16] M. Grotte, F. Duprat, D. Loonis, and E. Pietri, *Int. J. Food Prop.* **4**, 149 (2001).
- [17] S. Stal and M. Spira, in *Plastic Surgery*, edited by S. J. Aston, R. W. Beasley, and C. H. Thorne (Lippincott-Raven Publications, Philadelphia, 1997)
- [18] A. K. Harris, P. Wild, and D. Stopak, *Science*, **208**, 177 (1980).
- [19] K. Burton, J. H. Park, and D. L. Taylor, *Mol. Biol. Cell* **10**, 3745 (1999).
- [20] A. Walter, H. Rehage, and H. Leonard, *Colloids Surf. A* **183–185**, 123 (2001).
- [21] The scaled Föppl–von Karman equations may be written as  $\epsilon^2 \nabla^4 w = [\phi, w]$ ;  $\nabla^4 \phi = -[w, w]$ , where  $[w, a] = a_{,xx} w_{,yy} + w_{,xx} a_{,yy} - 2a_{,xy} w_{,xy}$ , and  $\epsilon = h/L \ll 1$ . Using the following scalings:  $x \sim O(1)$ ,  $y \sim O(\epsilon^{1/2})$ ,  $\phi_{,xx} = T \sim O(1)$ ,  $\phi_{,yy} = b \sim O(\epsilon)$ ,  $w \sim O(\epsilon^{1/2})$  and expanding the solution in powers of  $\epsilon$ , we get (3) at  $O(\epsilon)$ .
- [22] R. da Silveira, S. Chaieb, and L. Mahadevan, *Science*, **287**, 1468 (2000).